Supporting Information

Solar evaporation for simultaneous oil-water separation and electricity generation with *Janus* wood-based absorbers

Yue Yang[1]*, Ze Fu[3], Qi Zhang[2]

[1]Jiangsu Key Laboratory of Chemical Pollution Control and Resources Reuse, School of Environmental and Biological Engineering, Nanjing University of Science & Technology, Nanjing 210094, China.

[2]National Laboratory of Solid State Microstructures, Collaborative Innovation Center of Advanced Microstructures, College of Engineering and Applied Sciences, Key Laboratory of Intelligent Optical Sensing and Manipulation, Ministry of Education, Jiangsu Key Laboratory of Artificial Functional Materials, Nanjing University, Nanjing 210093, China.

[3]Key Laboratory of Industrial Ecology and Environmental Engineering (Ministry of Education, China), School of Environmental Science and Technology, Dalian University of Technology, Dalian 116024, China.

Notes: Yue Yang and Ze Fu contributed equally to this work.

*E-mail: yangyue2022@njust.edu.cn

1. Experimental

1.1 Water evaporation performance under 1-sun irradiation.

The water evaporation rate was calculated by the following equation:

$$v = \frac{d\dot{m}}{S \times dt} \quad (1)$$

where ṁ is the mass of the evaporated water (g), S is the illuminated area. t is time, and v is evaporation rate (kg•m^{-2}•h^{-1}).

The energy conversion efficiency was defined as the following equation:

$$\eta = vh_V/C_{opt}P_0 \qquad (2)$$

where v denotes the evaporation rate ($v = v_{\mathrm{Light}} - v_{\mathrm{Dark}}$). v_{Light} and v_{Dark} are the evaporation rate under light and dark conditions, respectively. h_V refers to the water vaporization enthalpy in *Janus*-ACB, P_0 refers to the solar irradiation power of 1-sun (1 kW•m^{-2}), and C_{opt} is the optical concentration on the surface of *Janus*-ACB.

1.2 Characterization.

Scanning electron microscopy (SEM, Quanta 200 FEG) was used to analyze the morphology of the samples. Fourier transform infrared spectrum (FTIR) of the sample was obtained on KBr pellets on a spectrometer (Nicolet, Madison). X-ray photoelectron spectroscopy (XPS, VG ESCALAB250) was carried to analyze the elementary composition of samples. The light adsorption of samples was performed by the ultraviolet-visible-near-infrared spectrophotometer (UV-vis NIR spectra) equipped with an integrating sphere. FLIR E6xt infrared camera was used to take infrared photographs. Water contact angle of samples was tested on an optical contact angle & interface tension meter (SL200KB, Kino, USA). The electrical measurements were carried out by the Advanced Electrochemical System (PARSTAT 2273). The concentration of NaCl in the *Janus*-ACB after solar irradiation was measured by ion chromatograph (881 Compact IC pro, METROHM).

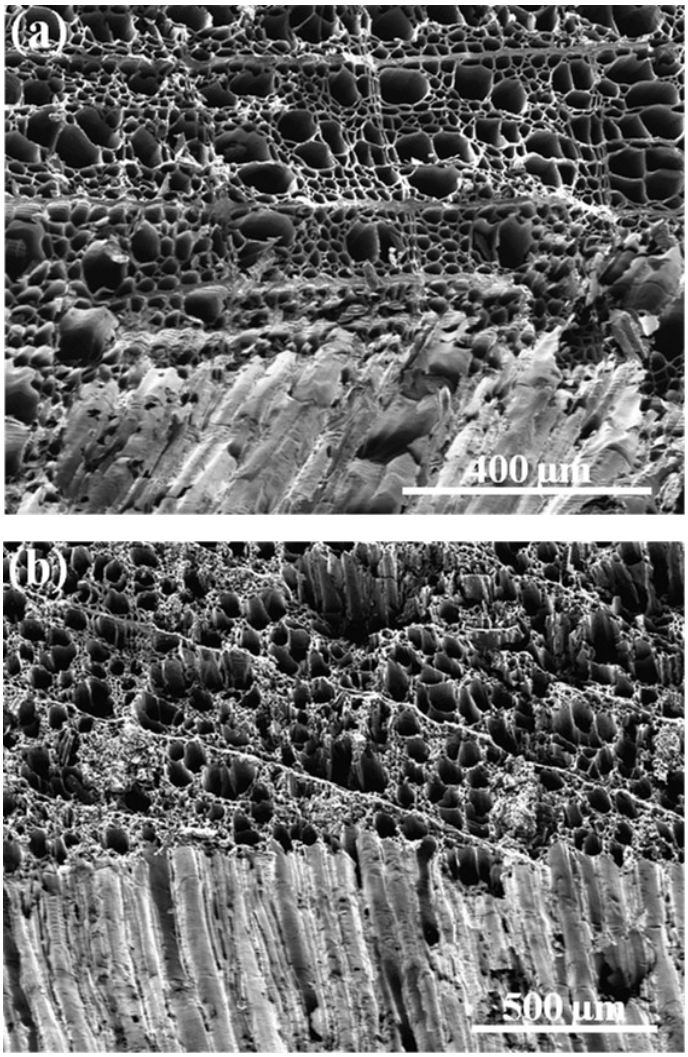

Figure S1. (a) Top-view and (b) bottom-view SEM images of the *Janus*-ACB, which demonstrates the interconnected wood channel structure from top to bottom.

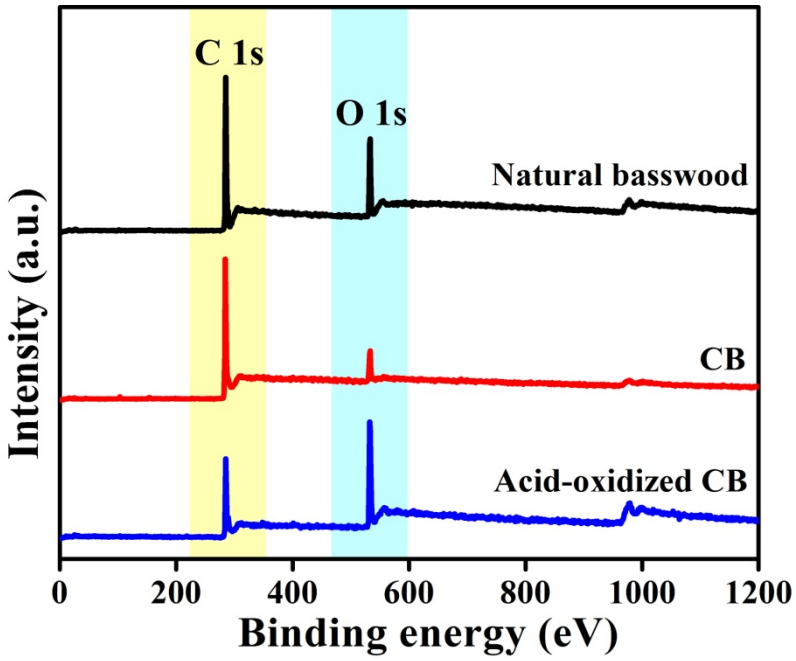

Figure S2. XPS spectra of the natural basswood, CB and acid-oxidized CB.

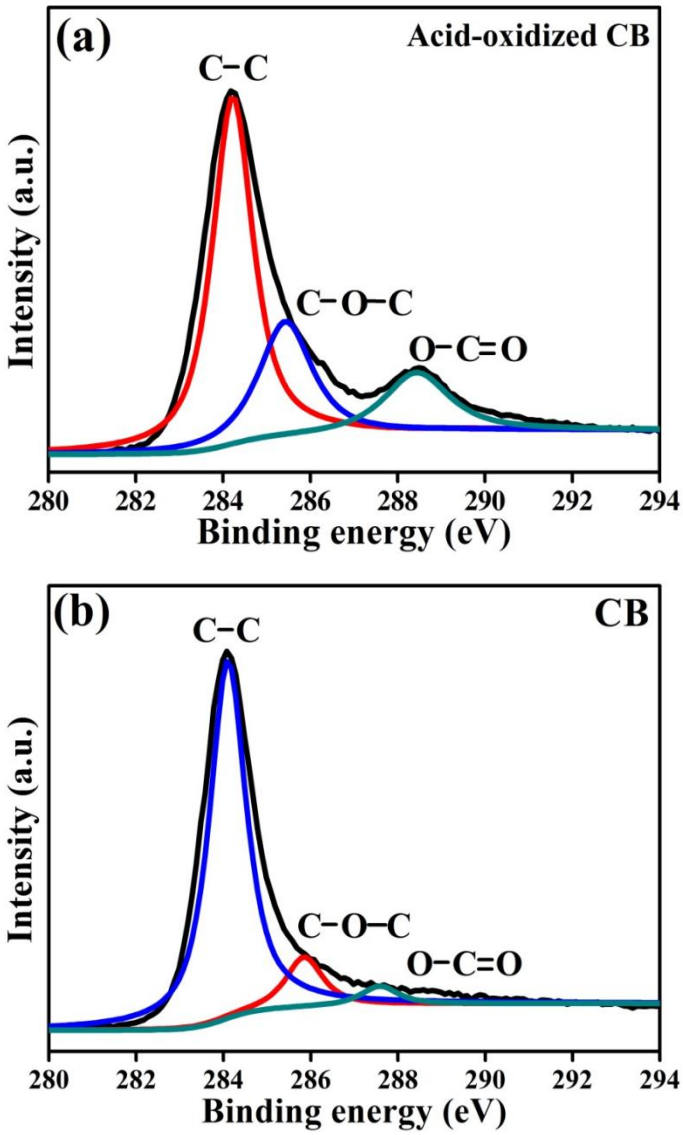

Figure S3. High-resolution XPS spectra of C 1s in (a) acid-oxidized CB and (b) CB.

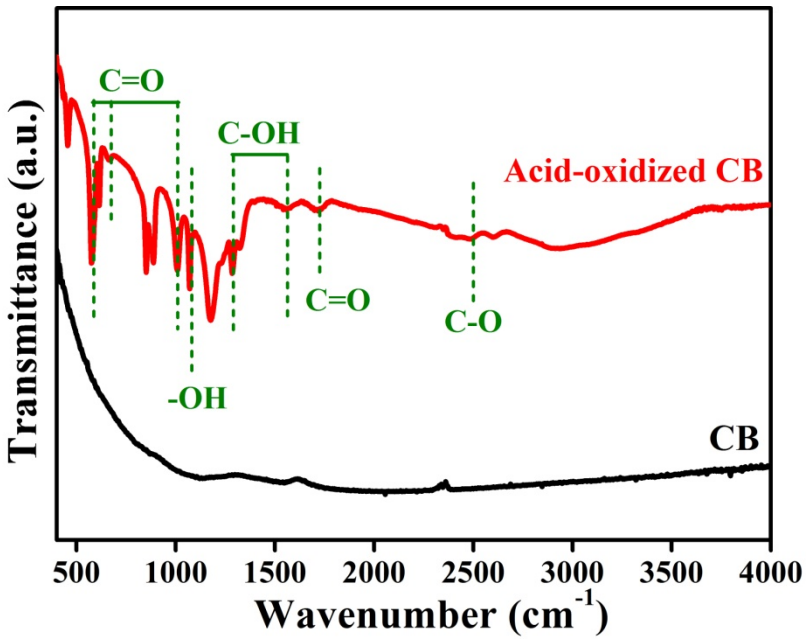

Figure S4. FTIR spectra of the CB and acid-oxidized CB.

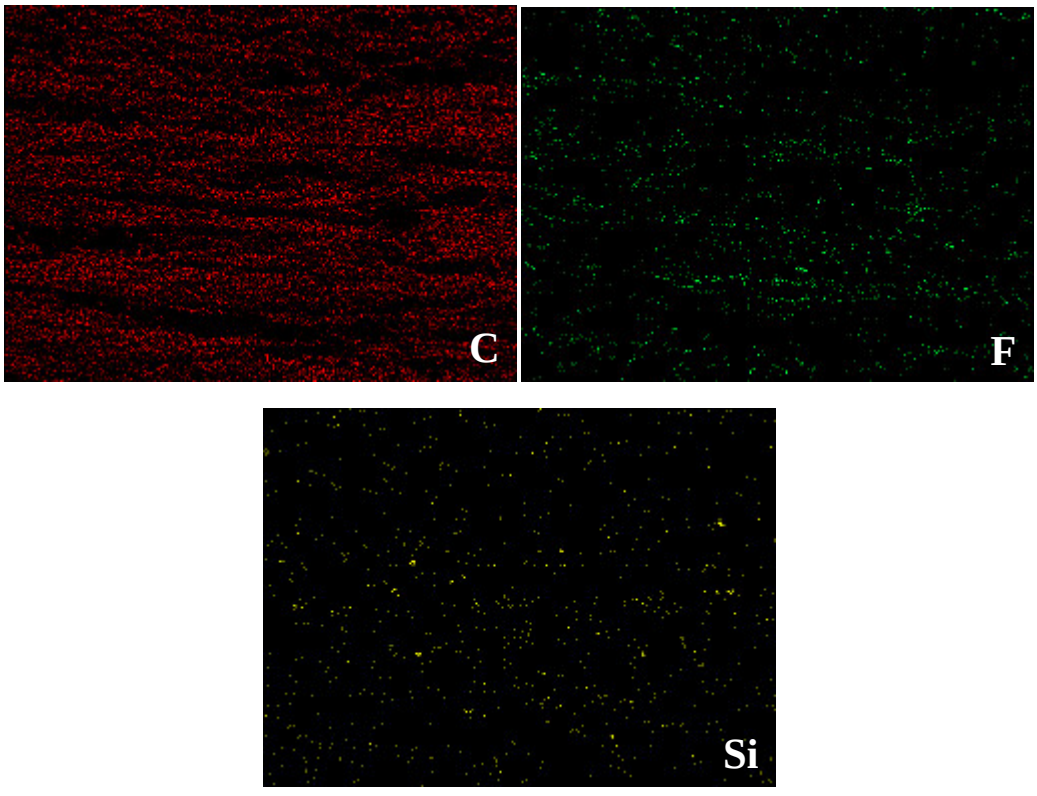

Figure S5. EDS images of the *Janus*-ACB top-surface.

Figure S6 illustrated the long-term stability test of the *Janus*-ACB evaporators in an oil-contaminated seawater. The evaporation efficiency of *Janus*-ACB evaporators still kept stable even after 10 h of solar irradiation compared with the evaporation efficiency at 1st hour, indicating a good oil resistance and salt resistance for the *Janus*-ACB evaporators.

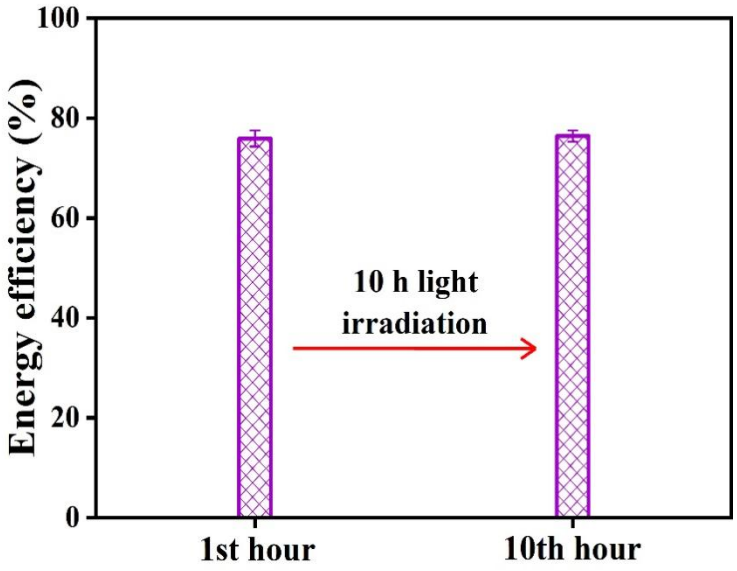

Figure S6. Long-term stability test of *Janus*-ACB evaporators in an oil-contaminated seawater with the solar irradiance for 10 h.

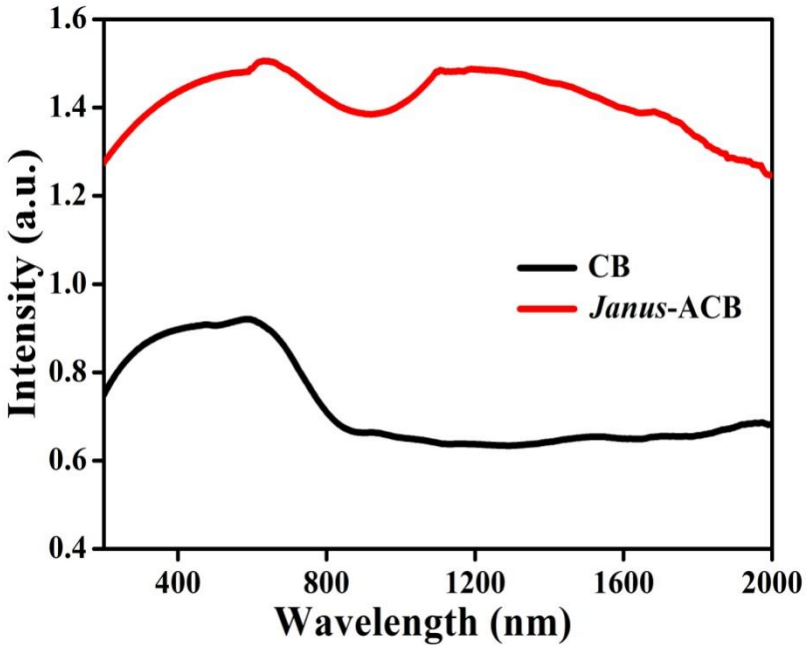

Figure S7. The comparison of light absorption intensity the *Janus*-ACB and CB after 10 h of solar irradiation.

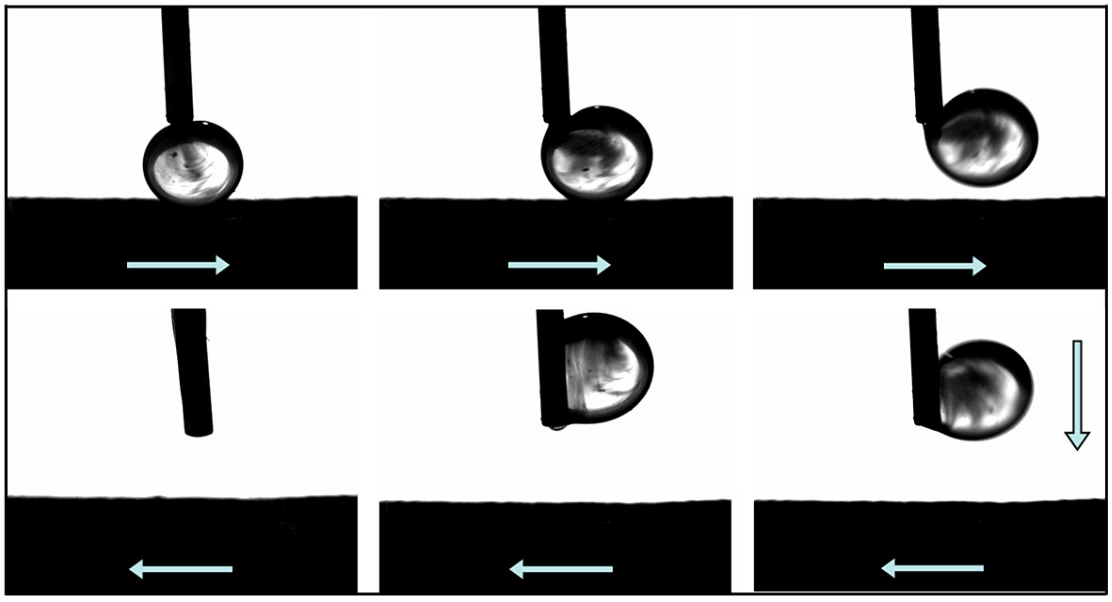

Figure S8. Image sequences of oil drops pressing on the bottom of *Janus*-ACB with time in water.

To evaluate the heat localization from *Janus*-ACB, the temperature across the evaporators was measured. The temperature of top-surface of *Janus*-ACB, bottom-surface of *Janus*-ACB, and water in the bottom of Dewar flask was carefully measured, as shown in Figure S9. The temperature was ~44.5 ºC for the top-surface of *Janus*-ACB after 3600 s under 1-sun irradiation. By contrast, the temperature was only 29.1 ºC and 23.5 ºC for bottom-surface of *Janus*-ACB and water in the bottom of Dewar flask, respectively. Therefore, the *Janus*-ACB can effectively convert the solar energy to thermal energy and only heat the water inside the *Janus*-ACB instead of heating the bottom bulk water, which is beneficial for efficient solar steam generation. All of the above results indicated that the great mass of heat energy from converted solar energy was consumed by the water inside the *Janus*-ACB, demonstrating a high-efficient energy utilization for our *Janus*-ACB.

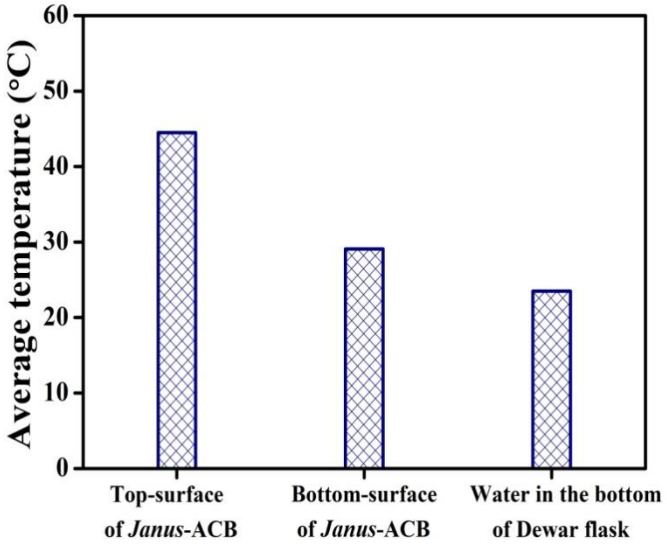

Figure S9. The temperature of top-surface of *Janus*-ACB, bottom-surface of *Janus*-ACB, and water in the bottom of Dewar flask.

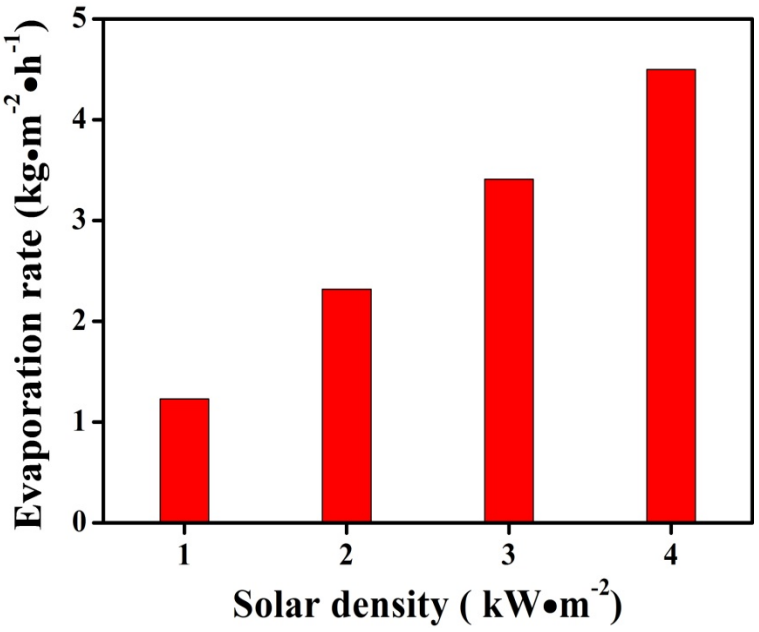

Figure S10. Water evaporation rate of *Janus*-ACB under 1.0 to 4.0 sun irradiation.

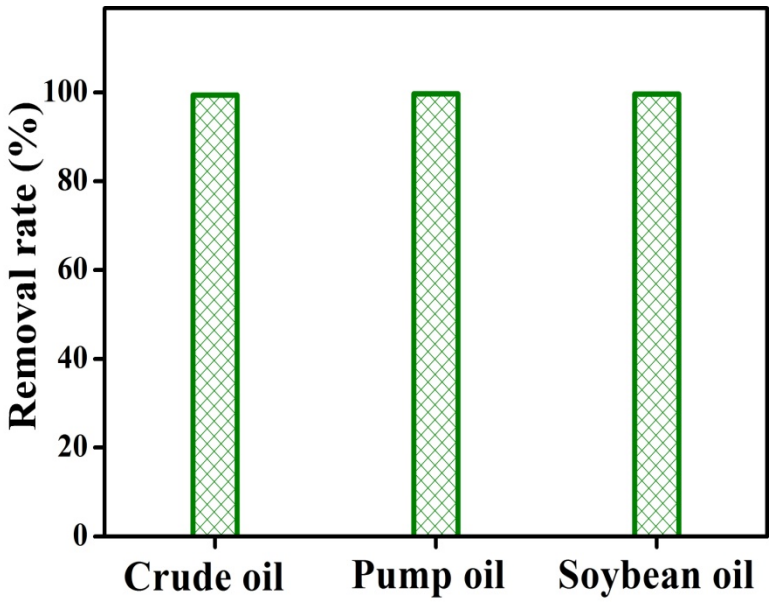

Figure S11. The oil removal rate of oily wastewater (crude oil, pump oil and soybean oil) after solar-driven separation.

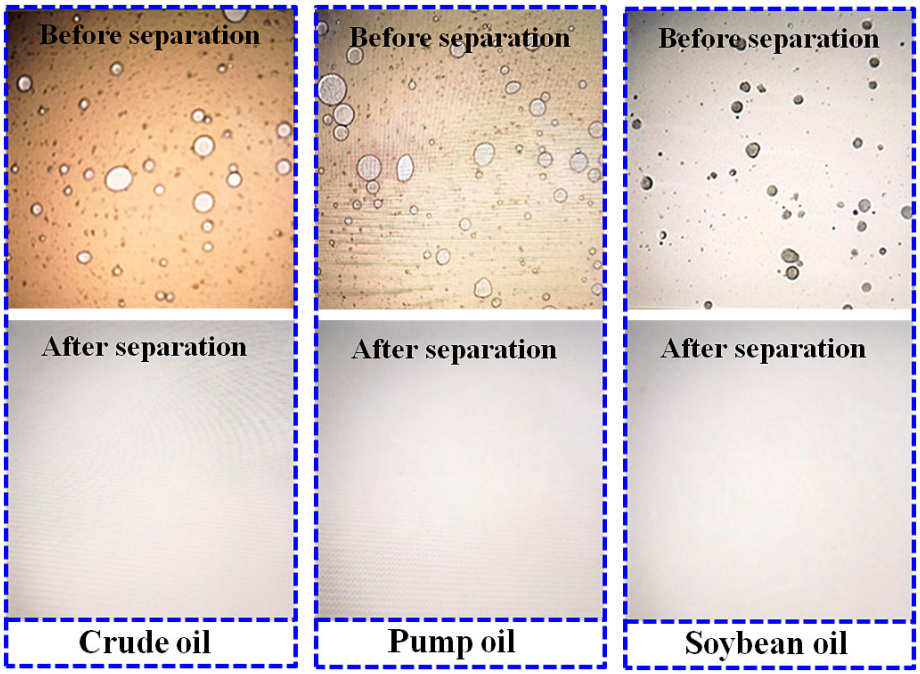

Figure S12. Microscopic photographs of oily wastewaters (crude oil, pump oil and soybean oil) before and after solar-driven separation.

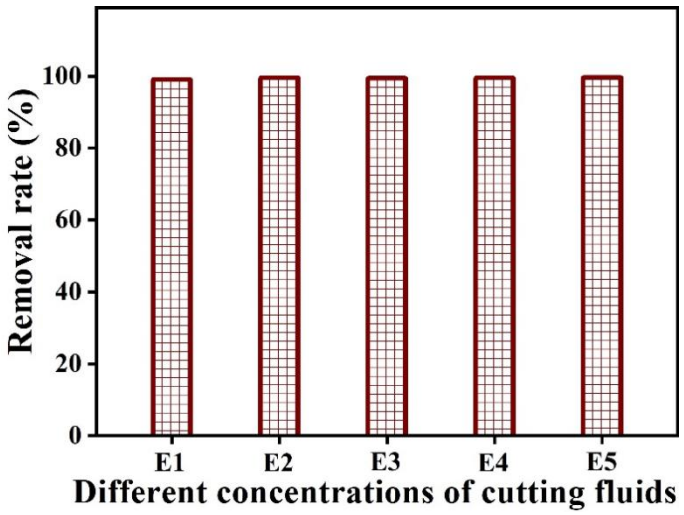

Figure S13. The oil removal rate of oily wastewater (cutting fluid emulsion) after solar-driven separation.

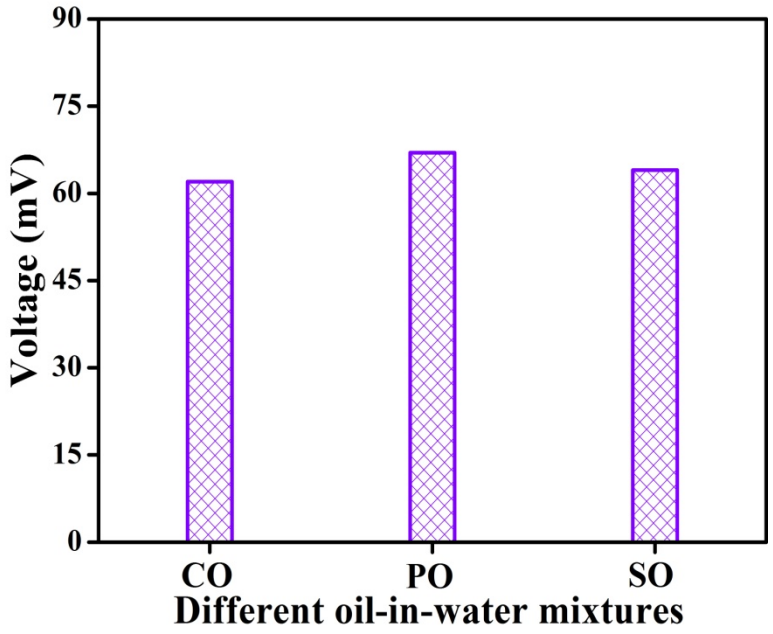

Figure S14. Voltage of *Janus*-ACB in different oil-in-water mixtures under 2-sun.

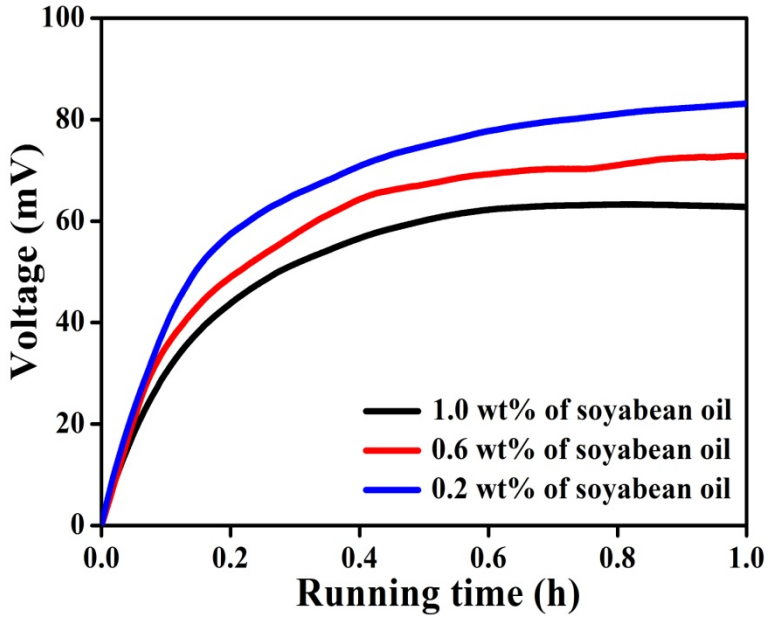

Figure S15. Voltage changes of *Janus*-ACB in different concentrations of oil-in-water mixtures under 2-sun.

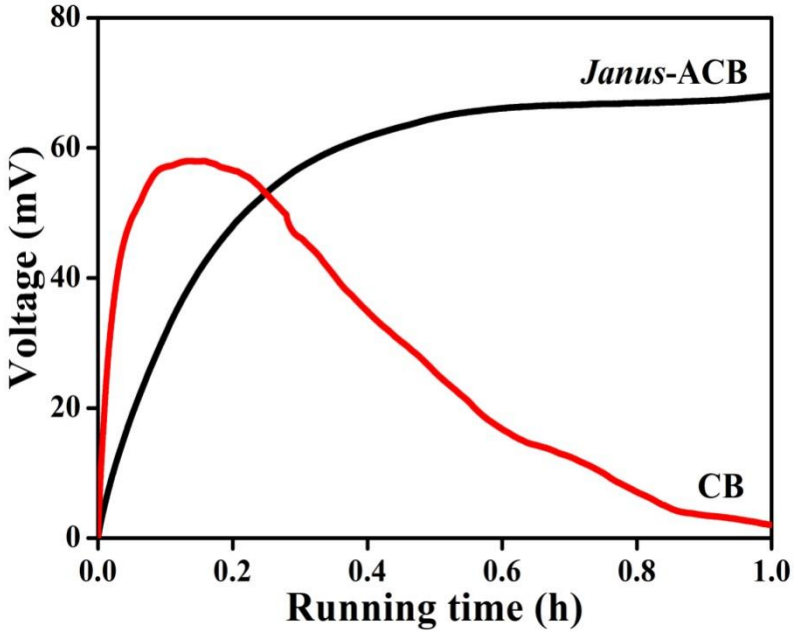

Figure S16. Comparing the voltage variation of CB and *Janus*-ACB under the same oil-in-water mixtures under 2-sun.

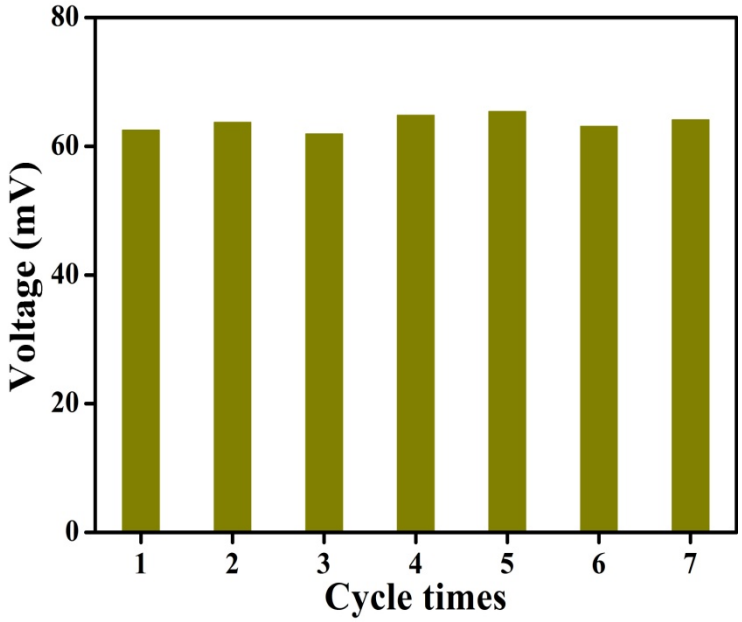

Figure S17. The voltage variation within 7 times cycle testing by using *Janus*-ACB.

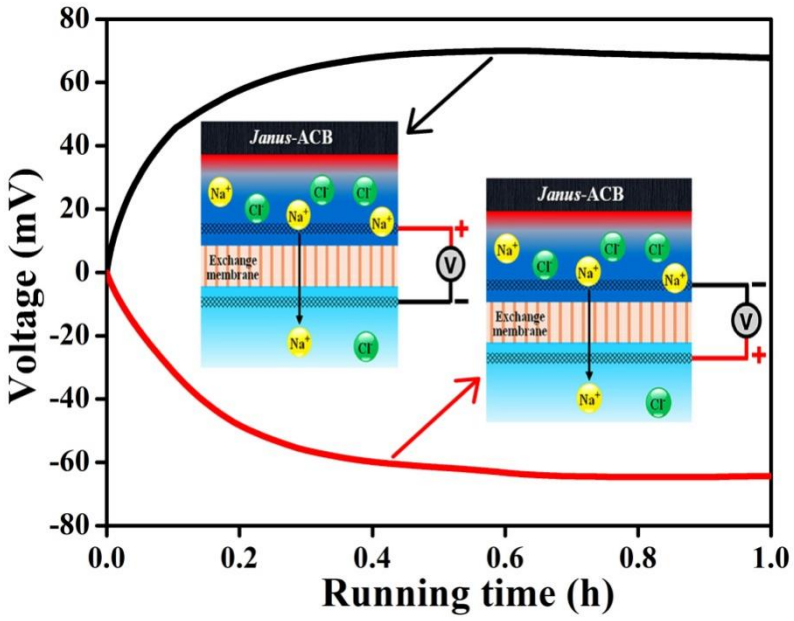

Figure S18. The electrical signal was reversed when the electric circuit connection was turned over without changing the Ti mesh connection. The red and black solid-line curves represented the corresponding voltage variations before and after turning over, respectively. Inset: Schematic diagram of the electric circuit before and after turning over.

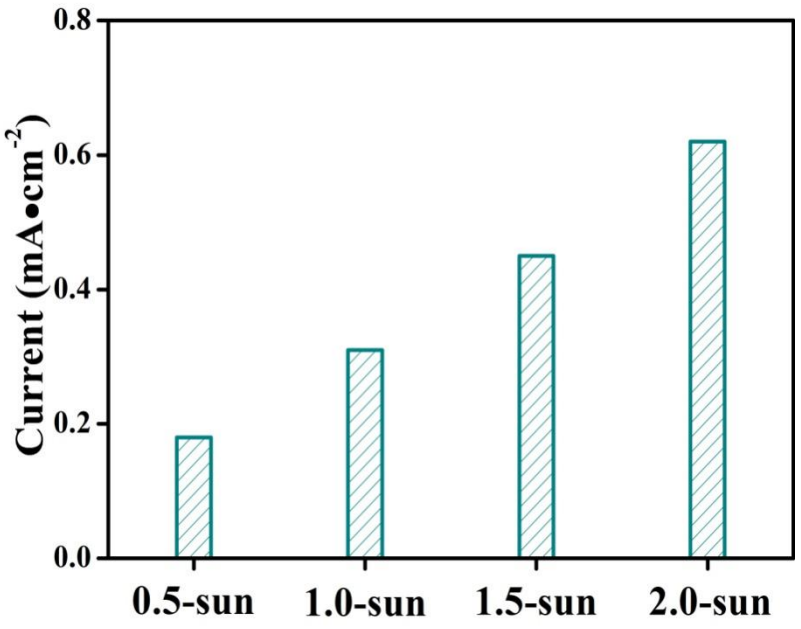

Figure S19. Current variations of *Janus*-ACB under different solar intensities. The current of *Janus*-ACB increased from 0.18 to 0.62 mA•cm^{-2} with the solar intensity increased from 0.5 to 2.0 kW•m^{-2}.

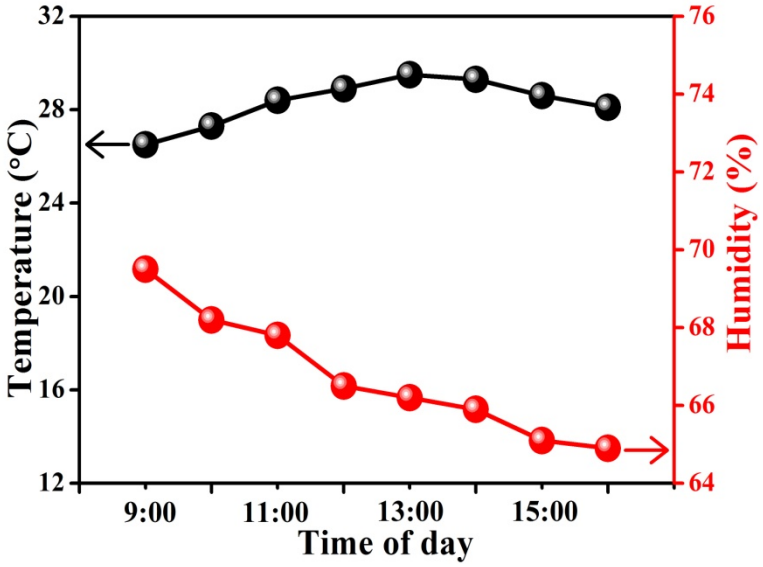

Figure S20. Variations of outdoor temperature and humidity over time within a day from 9:00 to 16:00.

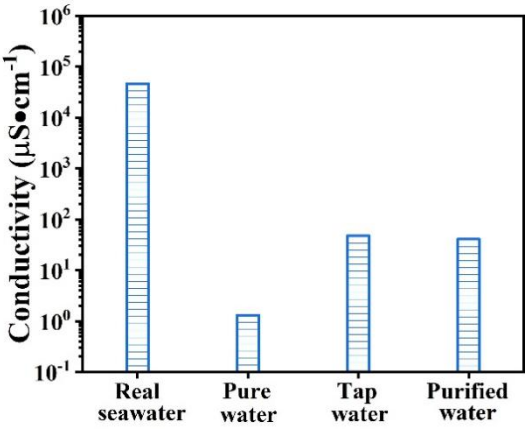

Figure S21. Evaluation of effluent quality by a portable multi-parameter analyzer (Multi 3430, Germany WTW).

These results showed a low conductivity value of purified oil-polluted seawaters with similar to that of tap water.